Макрогетероциклы
http://macroheterocycles.isuct.ru

DOI: 10.6060/mhc214085z

From Porphyrin Chemical Dimers to Complex Multicomponent Nanoassemblies: Some Rare Phenomena and Relaxation Processes

Eduard I. Zenkevich,[a@] Dietrich R. T. Zahn,[b,c] and Christian von Borczyskowski[b]

[a]*Belarussian National Technical University, 220013 Minsk, Belarus*
[b]*Chemnitz University of Technology, Institute of Physics, 09107 Chemnitz, Germany*
[c]*Chemnitz University of Technology, Research Center for Materials, Architectures and Integration of Nanomembranes (MAIN), 09107 Chemnitz, Germany*
[@]*Corresponding author E-mail: zenkev@tut.by*

Beginning from the first steps of a long standing and fruitful cooperation with Prof. G. Ponomarev and Dr. A. Shulga and inspired by their high professional level, a variety of highly organized multiporphyrin complexes of various morphology as well as nanoassemblies based on semiconductor quantum dots and porphyrins were formed based on a "bottom-up" approach. Using steady-state, time-resolved methods in combination with high spectral resolution experiments some specific and/or rare processes of excitation energy relaxation were found and discussed (fluorescence line narrowing and spectral hole burning, triplet-triplet energy transfer in dimers, photoinduced electron transfer at low temperature, distant superexchange charge transfer, etc.).

Keywords: Self-assembly, porphyrins, dimers, triads, energy transfer, charge transfer, inhomogeneous broadening of energy levels, long-distance superexchange photoinduced electron transfer, colloidal semiconductor quantum dots.

От химических димеров порфиринов к сложным мультикомпонентным наноансамблям: некоторые редкие явления и релаксационные процессы

Э. И. Зенькевич,[a] Д. Р. Т. Цан,[b,c] К. фон Борцисковски[b]

[a]*Белорусский национальный технический университет, 220013 Минск, Беларусь*
[b]*Технический университет Хемнитца, Институт физики, 09107 Хемнитц, Германия*
[c]*Технический университет Хемнитца, Центр исследования материалов, архитектур и интегрирования наномембран (МАИН), D-09107 Хемнитц, Германия*
[@]*E-mail*: *zenkev@tut.by*

В результате многолетнего и плодотворного сотрудничества с профессором Г.В. Пономаревым и доктором А.М. Шульгой и благодаря их высокому профессионализму на основе подхода «снизу-вверх» были получены высокорганизованные мультипорфириновые комплексы различной морфологии, а также наноансамбли на основе полупроводниковых квантовых точек и порфиринов. С использованием стационарной и время-разрешенной спектроскопии в комбинации с методами высокого спектрального разрешения были обнаружены и исследованы специфические и/или редкие процессы релаксации энергии возбуждения (выжигание спектральных провалов, Т-Т перенос в димерах, фотоиндуцированный перенос электрона при низких температурах, дистанционный перенос заряда по механизму суперобмена и т.д.).

Ключевые слова: Самосборка, порфирины, химические димеры, триады, перенос энергии, перенос заряда, неоднородное уширение энергетических уровней, дистанционный фотоиндуцированный перенос электрона по механизму суперобмена, коллоидные полупроводниковые квантовые точки.

Introduction

At the moment, the process of molecular self-assembly is considered as a fundamental phenomenon leading to the creation of targeted nanostructures with material properties on all scales through the organization of designed molecular or inorganic building blocks exhibiting proper intra- and intermolecular interactions along with the parallel control of the solution assembly pathways to yield the desired structural outcome.[1–6] In this respect, the designed self-organization process in solutions and solid state, the information necessary for the process to take place, and the algorithm that the process follows must be stored in the components and be operative via selective molecular interactions (including hydrogen bonding, coordination bonding, electrostatic and donor-acceptor interactions, and metal-ion binding[1,4]). Thus, such systems may be considered as programmed molecular or supramolecular complexes that generate organized entities by following a defined plan based on molecular recognition events.[2] The photophysical/photochemical study of self-organized systems is the subject of nanophotonics and biophotonics, which play a pivotal role in advancing nano/bio/info technology by creating new interfaces between multiple disciplines.[7] In-depth understanding of structure-function relationships for various self-organized nanoassemblies is essential for a rational design and development of functional nanoagents and nanodevices.[8]

Interestingly, nature, through billions of years of evolution, is an excellent place to find inspiration and ideas for molecular assembly. For instance, the most important and interesting example is natural photosynthesis of plants, algae, and bacteria. In those the generation of complex, multicomponent three-dimensional structures (based on chlorophylls as one of the most abundant organic pigments on the earth) involve intramolecular, as well as intermolecular and interfacial interactions.[9–12] The photosynthetic system is one of the finest pieces of nanoscale molecular machinery, wherein nature utilizes self-assembly principles to form multicomponent arrays of chlorophyll molecules and other organic substances that are capable for directed, very fast and efficient energy transfer (ET) among light-harvesting pigment-protein antenna complexes to the photochemical reaction center, where the energy of excited states is converted into a stable transmembrane charge separation through a sequence of photoinduced electron transfer (PET) reactions. Up to now the elucidation of the mechanisms and dynamics of ET processes in light-harvesting antenna complexes *in vivo* as well as the intrinsic peculiarities of PET events, such as charge separation and charge recombination of the product ion pair state, still remain the most fundamental and important problem.

From a practical standpoint, supramolecular bottom-up self-assembly based on tetrapyrrolic compounds is used to mimic these natural relaxation pathways and, additionally, offers an elegant solution to explore these principles in order to design perspective nanostructures possessing novel potential applications in improved drug delivery systems, photodynamic therapy, photovoltaic cells, optoelectronic memory, multimolecular architectures for information storage, and highly efficient catalysts.[13–23] The choice of tetrapyrrolic compounds for the formation of multimolecular systems with efficient ET or PET processes seems to be attractive because of the following reasons: (1) the similarity to the natural photosynthetic pigments; (2) tunable spectral-kinetic parameters that are easily controlled by various central metal ions or side substituents; (3) controlled redox properties and high photoreactivity; (4) relative stability as a host framework for organic guest molecules; and (5) relatively easy synthetic accessibility and the possible structural variability.

In fact, the formation of a variety of conformationally restricted, structurally and energetically well-defined multiporphyrin assemblies is based on the combination of two principally different synthetic strategies.[1] One approach utilizes the covalent linkage through spacers of various nature and the flexibility between supposedly essential components. The other, more common approach is based on non-covalent interactions of various kinds (electrostatic interactions, hydrogen bonds, and the coordination chemistry of transition metals). Noteworthy, the challenge remains for the design and investigation of new types of multiporphyrin complexes with well-defined geometry and predicted optical and physico-chemical parameters, since the optimal molecular arrangement for various applications in nanotechnology has not yet been realized. Correspondingly, both synthetic methodologies, each with its advantages and disadvantages, continue to supply a large variety of new multicomponent arrays with pronounced ET and PET properties. The resulting crossover has provided novel principles and concepts in physico-chemistry such as molecular recognition, self-organization, regulation, cooperativity, and replication. The significant interest of numerous scientific groups in this direction has been devoted to the design and investigation of tetrapyrrole compounds that fold or assemble predictably in order to form multicomponent well-defined arrays. A large body of interesting and important results obtained in this field of supramolecular chemistry was presented and discussed in a lot of comprehensive reviews (*e.g.*[3–5,13,14,19]) and numerous articles (*e.g.*[15–18,24]).

The history of the covalently linked porphyrin macrocycles begins since 1972 by the investigations devoted to the synthesis and study of the energy transfer in covalenly linked metalloporphyrins.[25] After that within the next decade construction strategies were used for assembling various dimers of tetrapyrrolic macrocycles via predictable chemical engineering of all desirable components (*e.g.* abroad publications presumably [26–29]). In the former Soviet Union the first results on systematic chemical approaches in the field of porphyrin chemical dimers appeared in 1982–1983.[30–32] It should be noted, that in those times the leading role in this area belonged, without any doubts, to the closely cooperating Prof. Geliy V. Ponomarev (Scientific Research Institute of Biomedicine Chemistry named after V.N. Orekhovich, Moscow, Russia) and Dr. Alexander M. Shulga (Institute of Physics, Natl. Acad. Sci, of Belarus, Minsk, Belarus). They succeeded to elaborate original routes of the synthesis and identification (using experimental and quantum chemistry abilities) of novel porphyrin dimers with various chemical spacers between tetrapyrrolic macrocycles.[31–35] Geliy and Alexander were always ready to share their ideas with others being able to use their

ability to explain complex chemical questions in simple, understandable terms, sometimes accompanying their explanations with a very humorous style. They were always full of energy and inspired others with their deep knowledge and enthusiasm for science. Perhaps more important than their insight into the chemistry of porphyrin dimers were their friendly relations with physicists (theoreticians and spectroscopists) both in Russia and Belarus. As a result within this cooperation, considerable progress was achieved in the study and analysis of experimental and theoretical results on structural properties and the deactivation of locally excited S_1 and T_1 states (including ET and PET processes) for porphyrin and chlorin chemical dimers (and corresponding metallocomplexes) with various spacers, taking into account various additional effects such as interchromophoric interactions, steric hindrance effects, axial extra-ligation, NH-tautomerism, and exchange d-π effects.[36–53] Owing to this physico-chemical fruitful cooperation the results of Soviet school in chemistry and photophysics of chemical dimers of tetrapyrrolic compounds were in one line with those being obtained elsewhere.[13–15,54,55]

G.V. Ponomarev (1941–2021)

The contribution of G. Ponomarev and A. Shulga to the research followed by the further development of the ways for the formation of large functional multiporphyrin arrays resulted in a new stage of our scientific activity. Within the German-Belarus scientific cooperation we have realized a simple and yet potentially versatile strategy for the formation of highly organized and relatively rigid multimolecular tetrapyrrole nanoassemblies based on the combination of covalent linkage and non-covalent interactions in solutions and polymeric (PMMA) films.[56–71] The first step presents itself as a covalent stage, where precursor molecular blocks such as Zn porphyrin or Zn chlorin chemical homo- or heterodimers with a covalent linkage of various nature ($-CH_2-CH_2-$ or a phenyl ring in *meso*-position) as well as chemical trimers of Zn octaethylporphyrins with phenyl spacers in *meso*-positions were synthesized. Additionally, various types of electron acceptors (quinone, anthraquinone, pyrromellitimide, NO_2 group) could be covalently linked to these dimers by flexible or rigid spacers. In the second step covalently linked dimeric or trimeric porphyrins (with/without electron acceptors) were self-assembled with pyridyl containing porphyrin or chlorin extra-ligands through non-covalent binding interactions between the central Zn ions of the porphyrin macrocycles and the N atom of the pyridyl-like extra-ligand (N-pyr). It is well known from chemical literature that the Zn^{2+} ion has vacant d^{10} orbitals while the heteroatom N-pyr is a good e-donor having an unshared electron pair. Correspondingly, in this case a "key-hole" principle is realized via one- or two-fold non-covalent coordination Zn….N-pyr with a perpendicular disposal of the extra-ligand with respect to the porphyrin macrocycle plane. Using comprehensive experimental studies (steady-state and time-resolved data) in combination with quantitative theoretical analysis carried out for well-defined self-assembled multiporphyrin arrays it was proven that photoinduced relaxation processes show complex energy and electron transfer dynamics, depending on the nanoassembly geometry, redox and photophysical properties of the interacting subunits as well as on the temperature and polarity of the solvent. As a result, more than 50 objects (including monomeric precursors, porphyrin chemical dimers and trimers, triads, pentads, and octads obtained and prepared with participation of Geliy and Alexander) were systematically studied and characterized. Nevertheless, it is evidently seen that multiporphyrin donor-acceptor nanoassemblies still remain to be attractive systems for the study of energy and/or electron transfer processes (mimicking the primary photosynthetic events) as well as for the design of nanoscale devices in nanoelectronics.

Inspired by the work on self-assembled multiporphyrin arrays, we ,with the direct participation of Alexander Shulga, succeeded in the direct labelling of semiconductor quantum dots (QDs), CdSe/ZnS or CdSe, with pyridyl-substituted porphyrins, $H_2P(m\text{-}Pyr)_n$ (n = 1, 2, 3, or 4), based on the coordination of the pyridyl N lone pair with Zn or Cd atoms of the QD surface.[72–74] This approach is considered as the "bottom-up" non-covalent strategy for the formation of organic-inorganic nanomaterials in solutions and solid state.[75] Using a combination of ensemble and single molecule spectroscopies of "QD-Porphyrin" nanoassemblies, we showed that single functionalized molecules can be considered as extremely sensitive probes for studying the complex interface physics and chemistry and related exciton relaxation processes in QDs.[76–84] It was quantitatively shown that the major part of the observed QD photoluminescence (PL) quenching in nanoassemblies is caused by electron tunneling to the QD surface in conditions of quantum confinement, which is influenced by the attachment dynamics of porphyrin molecules. In these nanoassemblies, Foerster-type energy transfer (FRET) QD→dye is often only a small contribution to the PL quenching and is already effectively suppressed in slightly polar solvents. This fact is often overlooked in the literature. In addition, we like to point out, that the properties of "QD-Porphyrin" nanoassemblies are not only interesting in themselves, but also provide a valuable tool to study surface related phenomena in QDs on an extremely low level of surface modification thus providing the data for the further development of defined multi-component structures for exploitation as artificial

light-harvesting complexes, electro- and photochemical devices, or nanosensors.

A.M. Shulga (1941–2014)

It gives us a greatest pleasure to present this Tribute for the *Macroheterocycles* issue honoring Prof. Geliy V. Ponomarev and Dr. Alexander M. Shulga for their fruitful and useful contributions within several decades in many disciplines including chemical engineering, physical chemistry, biophysics, and medicine. The intention of this paper is not a thorough description of specific structural aspects and all relaxation processes in nanoassemblies under study, which one could find in our cited references describing also chemical approaches, the detailed spectral-kinetic information, as well as theoretical models and details of the experimental setups used. Of course, we do not pretend to be entirely comprehensive in this respect, as far as many hundreds of excellent and important papers devoted to the chemistry and photochemistry of multiporphyrin arrays appeared in the last decade. Rather the present paper should be considered as a more comparative overview and description of some rare phenomena and relaxation processes for nanoassemblies of various morphology containing tetrapyrrolic subunits, which were obtained by us in some cases for the first time or using specific spectroscopic experimental methods. These findings would not be so remarkable and known in the world without Geliy's and Sasha's input providing an additional background for the further development of defined multicomponent structures for their exploitation as artificial light-harvesting complexes, electro- and photochemical nanodevices, nanosensors, *etc*.

Porphyrin Cyclodimers: Site-Selective Spectroscopy at 4.2 K and Time-Resolved Measurements

Site-selection spectroscopy of covalently linked dimers of tetrapyrrolic compounds with known structural parameters intermediate between monomeric chromophores and aggregated complexes *in vivo* and *in vitro* represents a convenient background to study specific spectral effects and interchromophoric interaction processes between coupled subunits. In our experiments the method of fluorescence line narrowing (FLN) of molecules in isotropic media was used.[51] This method is based on selective laser excitation within the band of 0-0 electronic transition in the absorption spectra of the compound at very low temperature (~4.2 K). Under such conditions the fluorescence spectra consist of narrow zero-phonon lines (ZPL) and frequency gaps separating them from the excitation line providing the frequencies of vibrations in the electronic ground state.[85]

Figure 1 shows that a 31,51-porphyrin cyclodimer includes one 3^1,5^1-cyclo-3^1-methyl-2,7,8,12,13,17,18-heptaehtyl-22*H*,24*H*-porphyrin molecule (OEP-cycle, a potential electronic excitation energy donor, D) and one 3^1,5^1-cyclo-3^1-exomethylene-2,7,8,12,13,17,18-heptaehtyl-22*H*,24*H*-porphyrin molecule (OEP-cycle=CH_2, a potential electronic excitation energy acceptor, A). Both subunits in the dimer were porphyrin free bases, Zn- and Cu-complexes. Quantum chemical calculations show that planes of the 3^1,5^1-cyclodimer subunits form an angle of approx. 78° with an intercenter distance R_{DA}=1.23 nm. The rigid structure of the cyclodimer results in a small overlap of p-electronic systems of their subunits, which in turn leads to almost unchanged visible absorption spectra and probabilities of intramolecular transitions of D and A comparable to the corresponding monomeric compounds. For the Zn-cyclodimer, weak dipole-dipole interaction of the dimer subunits ($V_{12} \leq 3$ cm^{-1}) manifests itself by effective quenching of the emission of D due to an ET process ZnOEP-cycle* → ZnOEP-cycle.

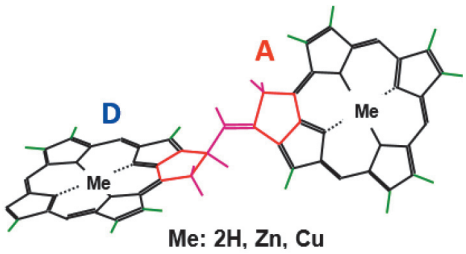

Figure 1. Chemical structure and calculated geometry of the 3^1,5^1-porphyrin cyclodimer

Scheme A of Figure 2 shows that upon excitation in the region of the $S_0 \rightarrow S_1$ electronic transition of solvated molecules the fluorescence spectrum consists of a set of narrow zero phonon lines (ZPLs, see curves F_m, F_a, F_c), which is caused by the sharp resonance between the excitation laser line and a narrow absorption band of one site and reflects the situation when a limited number of chromophores from the whole inhomogeneous spectral distribution are excited. It should be noted that the excitation into the region of the $S_0 \rightarrow S_2$ absorption band leads to FLN disappearance for individual monomers (spectrum b Figure 2B). At 77 K only the S_1 level of D (ZnOEP-cycle) plays an essential role in EM with a rate constant of $k_{EM}(S_1^D \rightarrow S_1^A) = 6.6 \cdot 10^{10}$ s^{-1}, while at 293 K the thermally activated S_2 state of D is involved in EM as well:

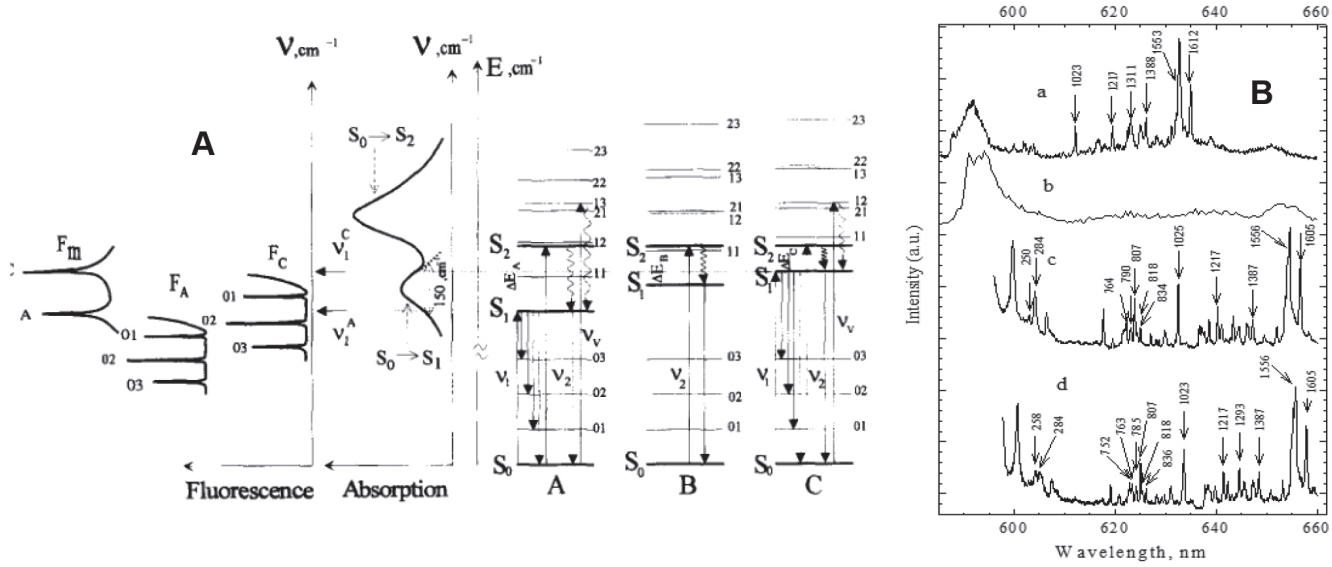

Figure 2. Schematic presentation of FLN spectra formation (A) and experimental fluorescence spectra (B) for metalloporphyrins with isocyclic substitution and their cyclodimers under conditions of an inhomogeneous spectral broadening at 4.2 K. A: Energy level diagram corresponds to three sites (A, B and C) excited into the vibrational sublevel manifold of the S_1-state. B: Fluorescence spectra of an equimolecular mixture ZnOEP-cycle+ZnOEP-cycle=CH_2 (a, $\lambda_{exc.}$ = 576 nm), the Zn-3^1,5^1-cyclodimer (b, $\lambda_{exc.}$ = 579 nm; d, $\lambda_{exc.}$ = 594 nm) and the Zn-3^1,3^1-cyclodimer (c, $\lambda_{exc.}$ = 594 nm) in a tetrahydrofuran- toluene mixture (3:1) at 4.2 K.

$k_{EM}(S_1^D \rightarrow S_1^A) = 4.1 \cdot 10^{10}$ s^{-1} and $k_{ET}(S_2^D \rightarrow S_1^A) = 1.1 \cdot 10^{10}$ s^{-1}. Good agreement of experimental and calculated data for the *D* fluorescence quenching via ET at 77 K indicates that the Foerster theory of inductive resonance is still applicable to weakly interacting porphyrin aggregates with an intercenter distance of 1.23 nm.

The effective ET in Zn-cyclodimers takes place even at 4.2 K. Under these conditions, the selective laser excitation within the band of the $S_0 \rightarrow S_1$ transition of *A* leads to the dimer fluorescence spectrum consisting of zero phonon lines, while the excitation into the $S_0 \rightarrow S_1$ transition of the donor subunit (ZnOEP-cycle) leads to the disappearance of the fluorescence line narrowing (Figure 2). The latter effect may be treated as the non-correlation of $S_{0D} \rightarrow S_{1D}$ and $S_{1A} \rightarrow S_{0A}$ transitions for different donor-acceptor pairs in ET processes (rate constant $k_{ET} \geq 10^{10}$ s^{-1}) caused by the inhomogeneous broadening of electronic levels at 4.2 K. The main conclusion is that in Zn-cyclodimers ET can involve differently polarized S_0-S_1 and S_0-S_2 transitions of A and A molecules, but in the case of dipole-dipole interactions at 4.2 K there is no exact correlation between the energies of electronic transitions of D and A subunits in the dimers, *e.g.* the D-A energy gaps are not constant. As a result, we observe the loss of selectivity followed by the disappearance of the fine structure in dimer fluorescence spectra.[47,49]

In the case of Cu-cyclodimers, fast intersystem crossing to the ^{2,4}T states with the rate constant of $k = 3 \cdot 10^{13}$ s^{-1} in both subunits containing central Cu ion prevents S-S ET between donor and acceptor (theoretical rate constant is $k_{ET}^{theor} < 4 \cdot 10^{10}$ s^{-1}). Nevertheless, a strong quenching of D phosphorescence is observed for these dimers at 77 K.[48] Bands of D detected in phosphorescence excitation spectra of A evidently show that this quenching is due to an exchange ET between T-levels of interacting subunits in the Cu-cyclodimer. In addition, phosphorescence spectra detected with a delay time θ = 3.8 ns evidently show the time scale for T-T ET realization (Figure 3).

In this case, the experimental value of the rate constant ($k_{ET}^{TT} = 2 \cdot 10^8$ s^{-1}) for T-T ET is much higher than the rate constant of the donor T-state deactivation ($k^0_T = 6.7 \cdot 10^3$ s^{-1}). Interestingly, the exchange T-T ET rate constant k_{ET}^{TT} is close to the values of rate constants characteristic for the deactivation of the S_1 level in H_2-cyclodimers ($k_S = (4–5) \cdot 10^7$ s^{-1}). Taking into account this fact it cannot be excluded that an exchange S-S EM may be responsible for the additional quenching of the donor fluorescence in the H_2-cyclodimers, where the dipole-dipole interactions are weak compared to those in the corresponding Zn-complexes.

We showed for the first time that an isocycle containing porphyrin free bases and chemical dimers on their basis (porphyrin 3^1,5^1- and 3^1,3^1-cyclodimers synthesized by Ponomarev and Shulga[31]) is characterised by the existence of an equilibrium mixture of two NH-tautomers and the spacing between S_0-S_1 transitions (Q_x bands) of the two tautomers reaches up to 380 cm^{-1}, while for S_0-S_2 transitions (Q_y bands) the spacing was measured to be up to 800 cm^{-1}. The principal difference was observed for the first time in the visible absorption spectra of NH-tautomers caused by the inversion of $Q_x(0,0)$ and $Q_y(0,0)$ band intensities, when NH-proton migration takes place.[37,41,43,44] In spite of the fact that the photoinduced NH-tautomerism does not compete with the deactivation of S_1 and T_1 states in these cyclodimers at 77 K due to the best resonance conditions for main long-wavelength tautomers of D and A ($J = 8 \cdot 10^{-15}$ cm^6·mol^{-1}),[44] the S-S ET in these cyclodimers results in the directed photoinduced transformations of the long-wavelength NH-tautomer 1 to the long-wavelength NH-tautomer 2 in the energy acceptor subunit A (OEP-cycle=CH_2) upon selective excitation of the donor molecule D(OEP-cycle). For these dimers at 77 K, the ET rate constants calculated in the frame of Förster

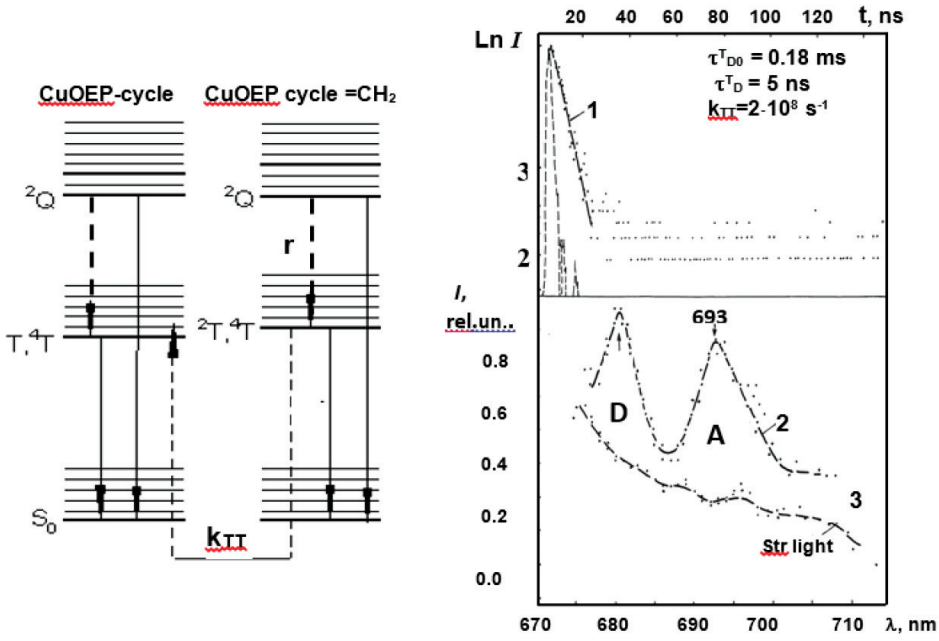

Figure 3. Scheme of the energy levels and relaxation processes in Cu-cyclodimers as well as the phosphorescence decay (curve 1, λ_{exc}=380 nm, λ_{regr}=680 nm) and instantaneous phosphorescence spectrum (2, delay time θ=3.8 ns, $\Delta t_{1/2}$= 2.5 ns) in tetrahydrofuran-toluene mixture (3:1) at 77 K.

theory, $k_{EM}(S_1^D \rightarrow S_1^A) = (0.1 – 5.7)\cdot 10^8$ s^{-1}, are noticeably lower than those obtained in the experiment, $k_{EM} = 1.9\cdot 10^9$ s^{-1}. This deviation may be associated with the manifestation of weak exchange interactions of the S-states, which were confirmed by the observation of T-T ET in Cu-cyclodimers (discussed above).

Ethane-Bisporphyrin Dimers: Site-Selective Spectroscopy and Spectral Hole Burning at 4.2 K

For ethane-bisporphyrins $(OEP)_2$, NMR ^{1}H studies and computer-aided structure simulation showed that their conformers relative to the spacer range from the fully eclipsed (intercenter distance R = 0.55 nm) to the fully staggered (R = 1.06 nm) (Figure 4). The fully staggered conformer has the lowest energy and exists at low temperatures.[34,39,42,45]

In numerous papers, dealing with porphyrin dimers, the regularities of ET process were studied mainly at room temperature and the limits of different theoretical models describing this phenomenon were evaluated under these conditions. In the case of symmetrical dimers $(OEP)_2$, the S_1 state is deactivated mainly through intersystem crossing to the T_1 state, where the excitation is lost via non-radiative processes. Dipole-dipole interactions between homodimer subunits (1.5 cm^{-1} ≤ V_{12} ≤ 11 cm^{-1}) lead to Foerster type ET between them with a rate constant $k_{ET}^{SS} = (0.15 – 13.5)\cdot 10^{10}$ s^{-1}, and ET without quantum losses is much faster than the other deactivation processes in this dimer ($k_{\Sigma} = (0.9 – 1.2)\cdot 10^8$ s^{-1}). As a result, at 293 K numerous "jumps" of excitation between the subunits within the S_1 state result in the "collapse" of fluorescence excitation spectra of homodimers compared to the corresponding individual monomers.[40,42]

At the same time ET at low temperatures including the liquid helium range is strongly influenced by the arising zero phonon lines and phonon side bands.[86–88] The shape of the absorption and fluorescence 0-0 bands of the molecular systems at low temperatures is basically determined by inhomogeneous broadening. The methods of fluorescence line narrowing (FLN) and spectral hole burning (SHB) make it possible to overcome the inhomogeneity and reveal the underlying sharp-line homogeneous spectra. High spectral resolution

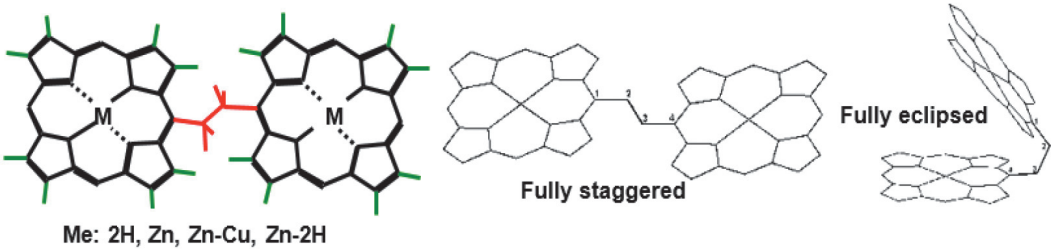

Figure 4. Chemical structures of ethane-bisporphyrin dimer $(OEP)_2$ and its fully staggered and fully eclipsed conformers.

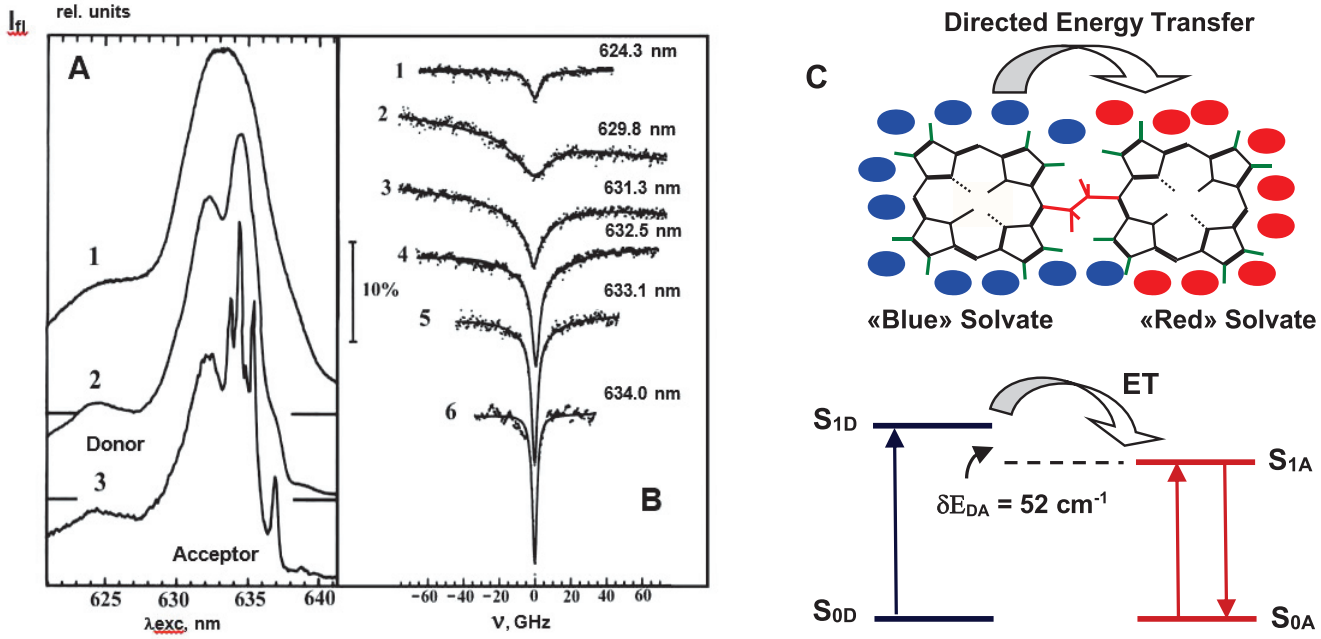

Figure 5. Spectral properties (A,B) and scheme of the directed energy transfer (C) for the ethane-bisporphyrin dimer $(OEP)_2$ in a tetrahydrofuran-toluene mixture (3:1) at 4.2–1.8 K. A: Fluorescence excitation spectra in the range of the Q(0,0) absorption band at various registration conditions, *e.g.* through wide-band cut-off filter, $\lambda_{trnsmit}$ >650 nm (1) and through a monochromator with slits of 1.1 (2) and 0.23 nm. B: Spectral holes at different wavelengths in the dimer fluorescence excitation spectrum. Solid curves are the least-squares fits by the sum of one (1,2,6), two (3,4,5) Lorentzian functions and a linear background. C: "Blue" and "Red" solvates are characterized by relatively higher and lower energies of the S_1 state of the same chemical monomers.

makes these methods very informative for studying the behavior of systems of various complexity.[85–88]

The influence of these effects on ET in porphyrin chemical dimers at liquid helium T was studied for the first time in our group using FLN and SHB methods.[49,51] In the case of ethane-bisporphyrins $(OEP)_2$ in a tetrahydrofuran-toluene mixture (3:1) at 4.2–1.8 K, some specific effects and regularities were observed (Figure 5).[49] 1) Upon wide-band excitation the full width at half maximum (FWHM) of the Q(0,0) band in the fluorescence spectra is by 1.5 times narrower than that for the Q(0,0) band in fluorescence excitation spectra. 2) Dimer fluorescence spectra with a set of narrow zero phonon lines (ZPLs) are observed only upon selective laser excitation on the long-wavelength side of the Q(0,0) absorption band (Figure 5A). 3) Upon SHB experiments on the long-wavelength side of the Q(0,0) absorption band, narrow holes (with FWHM values of δ_h=2.4 GHz) are registered, while upon SHB experiments on the short-wavelength side of the Q(0,0) absorption band the SHB efficiency decreases by one order of magnitude and the FWHM values for holes increase up to δ_h = 30 GHz (Figure 5B). It is well known that in the case of free-base porphyrins the hole-burning mechanism at low temperature is the photoinduced NH-tautomerism.[85,86] The tetrahydrofuran-toluene mixture (3:1) is a good low-temperature glassy matrice for SHB, as it yields a high Debye-Waller factor (*e.g.* 0.7 for $(OEP)_2$ when burning in the acceptor band). This indicates that the electron-phonon coupling is rather weak and it is possible to burn deep (up to 70 % of the initial value) holes in the absorption bands. An intense SHB results in a saturated zero-phonon line (with a laser-limited and power-broadened FWHM value) and a pseudo-phonon wing (FWHM = 31 cm^{-1}) shifted from the line to the red by 22 cm^{-1} (Figure 5B).

The first two effects are caused by two types of relaxation processes. In the conditions of an inhomogeneous distribution of the solvent molecules around the chemically identical porphyrin monomeric subunits in every $(OEP)_2$ dimer, the local solvent surrounding manifests itself in different positions of the locally excited S_1 states in the energy scale for the two halves of the dimer. It means that in the symmetrical homodimer $(OEP)_2$, one porphyrin macrocycle with higher S_1 state ("blue" solvate) acts as the energy donor (D), while the second one with lower S_1 state ("red" solvate) acts as the energy acceptor (Figure 5C). As a result, in the conditions of inhomogeneous broadening of energy levels, an irreversible ET "blue" solvate → "red" solvate in the dimer $(OEP)_2$ in the absence of a correlation between the 0-0 transitions in D-A pairs leads to the D emission quenching and the sensitization of the A emission. Such ET leading to the shortening of the fluorescence decay τ_S^D for the "blue" solvate is the main reason of the decreasing SHB efficiency and the rising FWHM values δ_h for holes (effect 3). Based on these quantitative results it was found that at 4.2 K, the rate constant of the directed ET between chemically identical macrocycles in the dimer $(OEP)_2$ is $k^{exp} = 1/\tau_S^D = 10^{11}$ s^{-1} and exceeds essentially the theoretical value $k^{theor} = (0.5 – 10)\cdot10^9$ s^{-1} at 77 K (calculated within the Förster model). This difference cannot be explained by the temperature dependence of the Förster ET mechanism, as commonly the non-radiative energy migration probability drops upon lowering of the temperature due to the decrease of the spectral overlap integral.

Low Temperature Photoinduced Electron Transfer in Porphyrin Triads

It is well known that processes of the photoinduced electron transfer (PET) in biological systems (*e.g.* photosynthetic objects) appear to be operative at cryogenic temperatures. In contrast, most of the artificial porphyrin- and chlorophyll-based D-A systems do not undergo effective PET in low-temperature solids due to the destabilization of the ion pair state.[15,29,54] Nevertheless, we showed[60,66–68] that this rare event such as the low temperature (77 K) photoinduced charge separation between porphyrin macrocycles may be observed in self-assembled triads if pentafluorinated porphyrin extra-ligands are used as interacting subunits. The structure of the triad based on the dimer $(ZnOEP)_2Ph$ (D) and a di-pentafluorinated porphyrin extra-ligand, H_2P-$(5F\text{-}Ph)_2$-$(m\text{^}Pyr)_2$ is shown in Figure 6.

In titration experiments, while the absorption spectra of the triad is the sum of the dimer and extra-ligand ones, in addition to the strong quenching of the dimer emission, an extremely low fluorescence of the fluorinated extra-ligand $H_2P(m\text{^}Pyr)_2$-$(5FPh)_2$ is observed. At 293 K in toluene, the fluorescence excitation spectrum (monitored via the extra-ligand emission at 717 nm) is identical in shape to that of the individual $H_2P(m\text{^}Pyr)_2$-$(5FPh)_2$, indicating that no fluorescence is sensitized via $(ZnOEP)Ph_2$ absorption, *i.e.* the ET process dimer → fluorinated porphyrin has a low probability in this triad V at ambient temperature. In this respect it should be mentioned that the individual fluorinated molecule $H_2P(m\text{^}Pyr)_2$-$(5F\text{-}Ph)_2$ is characterized by kinetic parameters of the excited S_1 and T_1 states ($\varphi_F = 0.07$, $\tau_S = 8.9$ ns and $\tau_T = 1.35$ ms), which are the same practically as for non-fluorinated porphyrin free bases.

It is known that pentafluorophenyl substituted porphyrin free bases are characterized by pronounced electron accepting properties (reduction potential $E_A^{red} = -0.85$ V in benzonitrile).[66–68] Thus PET process may be operative in this case. Direct pump-probe measurements for the triad under study reveal[66] (Figure 6) that the increased fluorinated extra-ligand bleaching at 510 nm is characterized by a time constant of ~700±200 fs and is attributed to the formation of the aradical anion of the extra-ligand and the radical cation of the dimer with the same characteristic time constants (Figure 6B). It means that in this triad at ambient temperature, the dynamics of the effective PET step is characterized by a time constant of 700±200 fs (Gibbs free energy $\Delta G^0 \approx -0.25$eV, the donor-acceptor distance $r_{DA} \approx 9.2$ Å), and the ET process dimer → fluorinated porphyrin has a low probability in these conditions. In addition, we showed[66,89] that this ET process remains very efficient upon temperature lowering down to 120 K ($k_{PET} \sim 10^{10}$–10^{11}s^{-1}) and competes with the singlet-singlet ET process from the dimer to the pentafluorinated extra-ligand. In the triad $(ZnOEP)_2Ph\otimes H_2P(5F\text{-}Ph)_2$-$(m\text{^}Pyr)_2$ PET is adiabatic at room temperature, while in a rigid solution at low temperature electron quantum tunneling may take place. Some reasons for the effective low-temperature PET in this case may be considered: i) the fluorinated porphyrin free base is strongly electron withdrawing and stabilizes a negative charge on its π-conjugated macrocycle; ii) the coordination of the electron-donating pyridyl rings helps to stabilize a positive charge on the Zn-dimer and thus lowers the energy of the radical ion pair state $^1(Dimer^+...Lig^-)$.

In this triad, because of the fast PET the direct population of the locally excited triplet T_1 state of the fluorinated extra-ligand cannot be populated via intersystem crossing S_1~~>T_1. Correspondingly, the effective formation of the extra-ligand low lying T_1 state (τ_T^0=6.4 μs in degassed

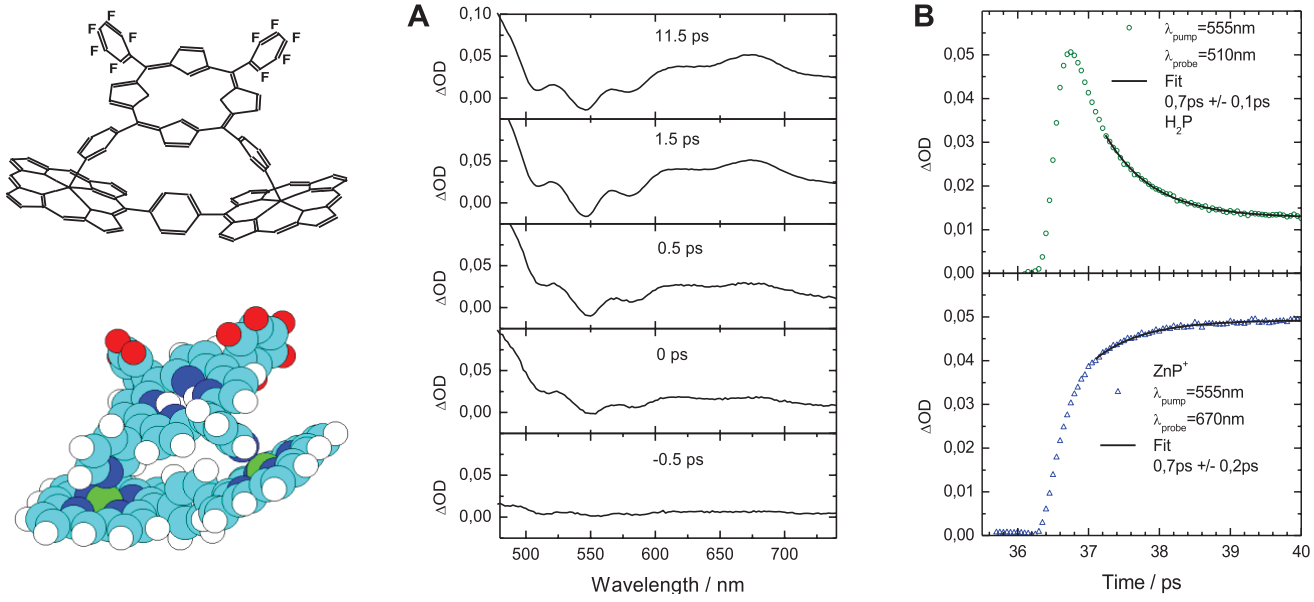

Figure 6. Optimized structure (HyperChem software package, release 4, semiempirical methods AM1 and PM3) and femtosecond pump-probe data for the $(ZnOEP)_2Ph\otimes H_2P(m\text{^}Pyr)_2$-$(5FPh)_2$ containing a di-pentafluorinated porphyrin extra-ligand, H_2P-$(5F\text{-}Ph)_2$-$(m\text{^}Pyr)_2$ in a toluene+methylcyclohexane mixture (1:10) at 293 K. Mark ⊗ denotes what subunits are coupled in the triad. A: Time-resolved transient absorption spectra at various delay times with respect to the exciting pump pulse at 400 nm. B: Time evolution of the transient absorbance for the fluorinated triad formed by the excitation at 555 nm and measured at 510 nm (top) and 670 nm (bottom).

solution) takes place from the upper-lying triplet or singlet radical ion pair states. Noteworthy, in the triad I, the decay of the low lying T_1 state of usual porphyrin extra-ligands is characterized by the significantly larger values of τ.[37,54,88,91] The τ_T shortening for the fluorinated extra-ligand in the triad (compared to T^0 = 1.2÷1.4 ms for the non-fluorinated one) may be caused by the mixing of an upper close-lying CT state with a locally excited T_1 state[54] thus leading to the rise of the non-radiative transitions T_1~~>S_0 in the acceptor subunit. The same conclusions were drawn also upon analysis of the relaxation dynamics for the self-assembled complexes based on chemical trimers of Zn-octaethylporphyrins with phenyl spacers in meso-positions, $(ZnOEP)_3Ph_2$ and containing $H_2P(m\text{^}Pyr)_2$-(5F-Ph)$_2$ or other fluorinated extta-ligands as far as the same tendencies are observed in fluorescence and excitation spectra of the last complexes.[69]

Superexchange Electron Transfer in Porphyrin Triads with Additional Electron Acceptors

The existence of an additional electron acceptor of non-porphyrin nature (quinone or pyromellitimide) covalently linked to the porphyrin chemical dimer $(ZnOEP)_2Ph$ leads to a more complex dynamics of the excitation energy relaxation in the corresponding triads.[68] The structure of the triad containing a dimer with a covalently linked quinone molecule (Q) and a porphyrin extra-ligand $(ZnOEP)_2Ph$-Q⊗$H_2P(m\text{^}Pyr)_2$-(iso-PrPh)$_2$ is presented in Figure 7.

Experimental studies of the triad $(ZnOEP)_2Ph$-Q⊗$H_2P(m\text{^}Pyr)_2$-(iso-PrPh)$_2$ show the following:[68] 1) The fluorescence of the dimer $(ZnOEP)_2Ph$-Q is strongly quenched due to PET process dimer → Q (~ hundreds of picoseconds[68]). Titration experiments indicate that the fluorescence spectrum of the triad is characterized by a substantial additional quenching of the dimer $(ZnOEP)_2Ph$ fluorescence and the emission consist mainly of the free-base extra-ligand fluorescence bands. In addition, the fluorescence quantum efficiency (φ_F) of the complexed extra-ligand $H_2P(m\text{^}Pyr)_2$-(iso-PrPh)$_2$ in the triad is essentially smaller as compared to that for the extra-ligand alone. 2) The fluorescence excitation spectrum (λ_{det} = 720 nm) even measured in pure toluene is almost identical in shape to that of the individual extra-ligand $H_2P(m\text{^}Pyr)_2$-(iso-PrPh)$_2$ and does practically not change in shape upon increasing solvent polarity (Figure 7B). 3) The rise of the solvent polarity leads to a fluorescence quenching of the complexed extra-ligand (by 1.3–1.4 times at 9 vol% of acetonitrile), while the dimer emission in this triad remains strongly quenched. 4) Based on TCSPC measurements (Figure 7C), an essential shortening of the fluorescence decays for the extra-ligand in Q containing triad was found (τ = 0.95 ns) compared to those for the same triads without Q (τ_0 = 7.7 ns). 4) In toluene at 293 K, femtosecond pump-probe experiments reveal that a non-radiative deactivation of the dimer locally excited S_1 state in the triad takes place within τ_1 < 6 ps.

These observed features for the Q-containing triad may be considered as evidence that the singlet-singlet ET dimer* → extra-ligand is slow compared to other pathways of the electronic energy deactivation of the excited dimer $^1(ZnOEP)_2Ph$*. Based on a quantitative comparison of steady-state and kinetic data obtained for the triad $(ZnOEP)_2Ph$-Q⊗$H_2P(m\text{^}Pyr)_2$-(iso-PrPh)$_2$ with those analyzed for the same triad without Q and available literature data for other covalently linked di-porphyrin-quinone systems,[90] it was concluded[67,68] that the non-radiative processes in this case may be realized with the participation of long-distance electron transfer mediated by superexchange interactions.[54,91,92]

The schematic energy level diagram of excited states for the triad under study (Scheme 1) shows the main relaxation pathways, which may be realized after the direct excitation of the dimer $(ZnOEP)_2Ph$. Being directly popu-

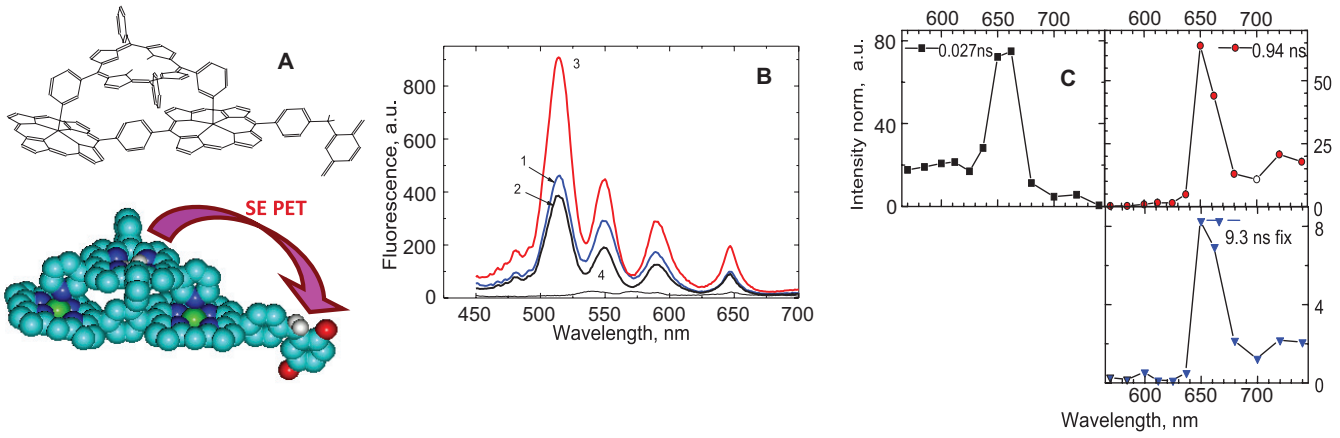

Figure 7. Optimized structure (HyperChem software package, release 4, semiempirical methods AM1 and PM3) (**A**), fluorescence excitation spectra (λ_{em}=720 nm, 293 K) of the triad upon increasing solvent polarity (**B**) and decay-associated spectra derived from the global analysis of 12 TCSPC time-resolved fluorescence measurements (**C**, toluene, 293 K, λ_{ex} = 546 nm) of the triad containing quinone $(ZnOEP)_2Ph$-Q⊗$H_2P(m\text{^}Pyr)_2$-(iso-PrPh)$_2$. For clarity, side alkyl substituents in pyrrole and phenyl rings are omitted. B: pure toluene (1) and + 9 vol% of acetonitrile (2); fluorescence excitation spectra of individual extra-ligand (3) and the dimer $(ZnOEP)_2Ph$-Q (4, multiplied by 10) in toluene at λ_{em}=720 nm.

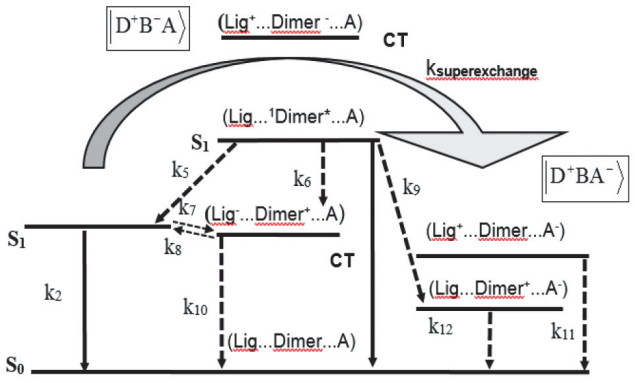

Scheme 1.

lated upon excitation at 545–555 nm in toluene at 293 K, the locally excited S_1 state (Lig...^{1}Dimer*...A) of the dimer $(ZnOEP)_2Ph$ in the triad may be deactivated as a result of the following non-radiative processes: (i) one-step PET to the ligand (rate constant k_6), (ii) one-step PET to Q (rate constant k_9), and (iii) low-probable ET to the ligand (rate constant k_5). In turn, the locally excited S_1 state of the extra-ligand may decay via two non-radiative processes: (iii) long-distant superexchange PET to Q (rate constant $k_{superexchange}$), and photoinduced hole transfer (rate constant k_7).

As outlined in detail,[64,67,68] superexchange PET occurs because of coherent mixing of three or more states of the system (the superexchange model including the corresponding electronic coupling terms[91,92]). Correspondingly, the dimer $(ZnOEP)_2Ph$ plays the role of the bridge, which does not directly participate in the PET process but lowers the barrier for its realization. Distant donor D and acceptor A can exchange their charges through the bridge, that is a high-lying "spectator" state $|D^+B^-A\rangle$ mediates the electron transfer from a donor state $|D^*BA\rangle$ to the charge transfer state $|D^+BA^-\rangle$.

Bottom-up Approach for "Quantum Dot-Porphyrin" Nanoassemblies

Finally, keeping in mind the "bottom-up" approach based on self-assembly principles and inspired by Alexander's and Geliy's experience, we elaborated a strategy of the formation of organic-inorganic nanoassemblies containing colloidal semiconductor QDs of different types (CdSe/ZnS and Ag-In-S/ZnS) and porphyrin molecules with functionalized anchoring side substituents or charged groups.[72–84] Like for porphyrin self-assembled triads, the importance of the designed two-point interacting domain was also demonstrated upon formation of the CdSe/ZnS QD-porphyrin nanocomposites. Really, in the solutions containing CdSe/ZnS QDs and triads/pentads there is a dynamic competition between the QD and the dimer $(ZnOEP)_2Ph$ to complex with the porphyrin extra-ligand. In this case we showed[78] that if the complexation constants K_C are comparable for "QD-porphyrin" nanoassemblies and triads (K_C =1.5·10^7 M^{-1}) or pentads (K_C =1.6·10^7 M^{-1}), the QD PL quenching values $I(x)/I(0)$ should be smaller by ~2 times compared to the corresponding values obtained for the titration by individual H_2P extra-ligands (within the same molar ratio $x = [C_{porph}]/[C_{QD}]$ range).

It was observed that the addition of increasing amounts of the dimer $(ZnOEP)_2Ph$ to the mixture solution [QD + $H_2P(p\text{-Pyr})_4$] does not lead to a decrease of the QD PL relative intensity (Figure 8, curve 1). This effect is attributed to the fact that upon addition of the dimer, the quenching counterpart of the "QD-porphyrin" nanoassemblies, namely $H_2P(p\text{-Pyr})_4$, remains to be attached to the QD surface. On the other hand, it is seen that the fluorescence of anchored $H_2P(p\text{-Pyr})_4$ ligands is continuously quenched upon titration by the dimer (Figure 8, curve 2). It should be noted that upon comparative titration of solutions containing individual $H_2P(p\text{-Pyr})_4$ molecules at the same concentration like in the case of the mixture solution [QD + $H_2P(p\text{-Pyr})_4$], the $H_2P(p\text{-Pyr})_4$ fluorescence quenching is also observed

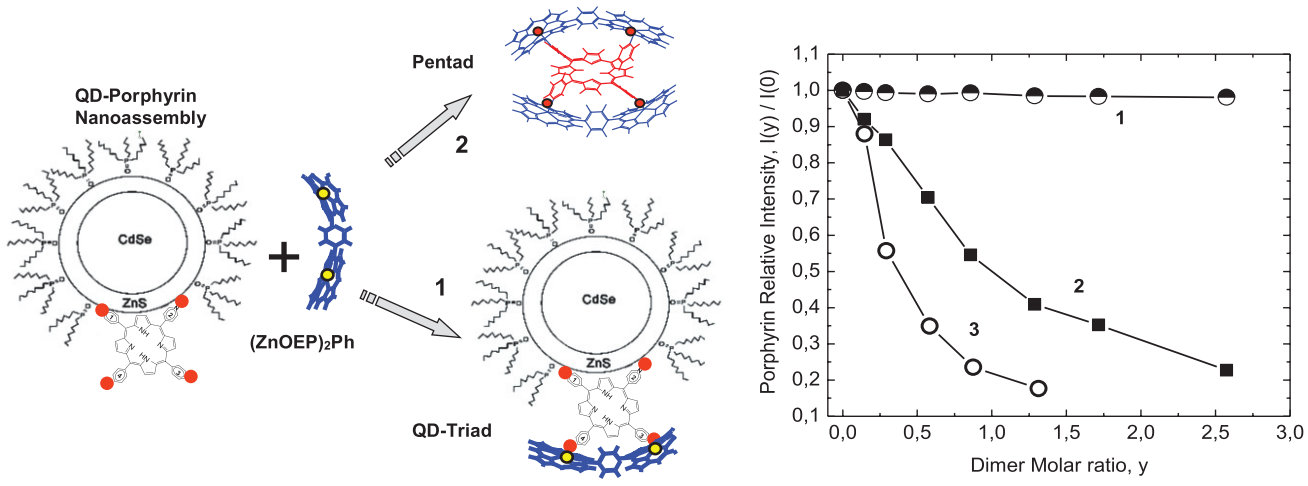

Figure 8. Left: Scheme of the competitive formation of "QD-Porphyrin triad" nanoassemblies (**1**) and self-organized pentads (**2**). Right: QD photoluminescence (curve 1, λ_{rec} = 481 nm) and extra-ligand $H_2P(p\text{-Pyr})_4$ fluorescence (curves 2, 3, λ_{rec} = 714 nm) relative intensities, $I(x)/I(0)$, as a function of the molar ratio y = [$(ZnOEP)_2Ph$] / [QD + $H_2P(p\text{-Pyr})_4$, x = 0.45] at constant molar ratio x = [$(ZnOEP)_2Ph$] / [$H_2P(p\text{-Pyr})_4$]=0.45 for solution with QDs (1 and 2) and for individual ligand $H_2P(p\text{-Pyr})_4$ (3). Toluene, 295 K, λ_{ex} = 465 nm.

(Figure 8, curve 3) being noticeably stronger with respect to a mixture solution containing QDs (curve 2). This difference is explained by the fact that in solution containing individual $H_2P(p\text{-Pyr})_4$ molecules only, the observed fluorescence quenching is caused by the formation of pentads $2(ZnOEP)_2Ph{\otimes}H_2P(p\text{-Pyr})_4$, in which the fluorescence of the extra-ligand is strongly quenched.[61,62,69,93]

These results may be explained as follows. Being anchored to QD surface via two adjacent *meso*-(*p*-Pyr) rings, the ligand $H_2P(p\text{-Pyr})_4$ may be attached with the dimer $(ZnOEP)_2Ph$ via coordination of the two central Zn ions of the dimer with *para*-nitrogens of two outer adjacent *meso*-(*p*-Pyr) rings (scheme in Figure 8). This complexation seems to be favorable because of the weakening of steric interactions of the dimer with neighboring TOPO molecules in the $H_2P(p\text{-Pyr})_4$ case. As a result, the triad $(ZnOEP)_2{\otimes}(p\text{-Pyr})_4H_2P$ should be formed on the QD surface. Moreover, according to experimental data,[55,61,62,69] the $H_2P(p\text{-Pyr})_4$ fluorescence in the triad should be less quenched with respect to the same extra-ligand emission in the pentad. It explains the observed smaller quenching effect for $H_2P(p\text{-Pyr})_4$ fluorescence found in mixture [QD + $H_2P(p\text{-Pyr})_4$] solution (Figure 8, curve 2, triad formation on QD surface) in comparison with that for the emission of individual $H_2P(p\text{-Pyr})_4$ solution (Figure 8, curve 3, typical pentad formation in a solution) at the same relative concentrations of the dimer.

Conclusions

Beginning from the first steps of our long standing and fruitful cooperation with Prof. G. Ponomarev and Dr. A. Shulga and inspired by their high professional level, a variety of highly organized multimolecular tetrapyrrole assemblies of various and known morphology were formed based on the combination of covalent linkage and non-covalent coordination interactions. Steady-state and time-resolved experiments show complex energy and charge transfer dynamics, depending on the nanoassembly geometry and composition, redox and photophysical properties of interacting subunits as well as on a temperature and polarity of the solvent. In addition to well-known photoinduced events (such as ET and PET processes) commonly observed in multiporphyrin nanoassemblies, some specific and/or rare processes of excitation energy relaxation dynamics were found and discussed: i) fluorescence line narrowing and spectral hole burning effects in porphyrin chemical dimers at liquid helium temperatures, which may be considered as precursors of single molecule spectroscopy studies;[93,94] ii) triplet-triplet ET in chemical dimers, which is still of interest now;[95] iii) unusual manifestation of NH-tautomerism in porphyrin cyclodimers; iv) fast femtosecond PET in triads with fluorinated extra-ligands, which is still effective at low-temperatures in rigid environments thus mimicking PET in reaction photosynthetic centers; v) distant superexchange PET with coherent mixing of the higher excited states of the bridge in porphyrin triads with covalently linked electron acceptors.

The same self-assembly approach (based on the non-covalent two-fold extra-ligation) was successfully extended to anchor (in a systematic and directed way) porphyrin molecules and porphyrin triads on semiconductor CdSe/ZnS quantum dot surfaces. It was also demonstrated that this approach can be employed to create nanosize hetero-nanoassemblies consisting of CdSe/ZnS QDs and porphyrin triads anchored on QD surfaces.

The results presented show that the design and self-assembly of organic/inorganic moieties into functional superstructures with vectorial energy relaxation dynamics are perspective for nanotechnology, supramolecular electronics, and nanobiotechnology.

Finally, thank all of them for joining together and taking the time to remember Geliy and Alexander.

Acknowledgements. This work was supported by the program BSPSR program “Photonics and Electronics for Innovations (2021–2025, Belarus)”, Volkswagen project No. I/79 435 (Germany) and Visiting Scholar Program of TU Chemnitz, Germany (E.Z., 2020–2021).

References

1. Lehn J.-M. *Angew. Chem., Int. Ed. Engl*. **1990**, *29*, 1304–1319.
2. Whitesides G.M., Grzybowski B. *Science* **2002**, *295*, 2418–2421.
3. *Self-Assembled Organic-Inorganic Nanostructures: Optics and Dynamics* (Zenkevich E., von Borczyskowski C., Eds.), Singapore: Pan Stanford, **2016**.
4. Pochan D., Scherman O. *Chem. Rev.* **2021**, *121*, 13699–13700.
5. Antipin I.S., Alfimov M.V., Arslanov V.V., Burilov V.A., Vatsadze S.Z., Voloshin Ya.Z., Volcho K.P., Gorbatchuk V.V., Gorbunova Yu.G., Gromov S.P., Dudkin S.V., Zaitsev S.Yu., Zakharova L.Ya, Ziganshin M.A., Zolotukhina A.V., Kalinina M.A., Karakhanov E.A., Kashapov R.R., Koifman O.I., Konovalov A.I., Korenev V.S., Maksimov A.L., Mamardashvili N.Zh., Mamardashvili G.M., Martynov A.G., Mustafina A.R., Nugmanov R.I., Ovsyannikov AS, Padnya P.L., Potapov A.S., Selektor S.L., Sokolov M.N., Solovieva S.E., Stoikov I.I., Stuzhin P.A., Suslov E.V., Ushakov E.N., Fedin V.P., Fedorenko S.V., Fedorova O.A., Fedorov Yu.V., Chvalun S.N., Tsivadze A.Yu., Shtykov S.N., Shurpik D.N., Shcherbina M.A., Yakimova L.S. *Russ. Chem. Rev.* **2021**, *90*, 895–1107.
6. Zhong H., Wang M., Ghorbani-Asl M., Zhang J., Ly K.H., Liao Z., Chen G., Wei Y., Biswal B.P., Zschech E., Weidinger I.M., Krasheninnikov A.V., Dong R., Feng X. *J. Am. Chem. Soc*. **2021**, *143*, 19992−20000.
7. Ohta K. *Physics and Chemistry of Molecular Assemblies*. Singapore: World Scientific, **2020**.
8. Bertino M.F. *Introduction to Nanotechnology*, Singapore: World Scientific, **2021**.
9. Cogdell R., Mullineaux C. *Photosynthetic Light Harvesting.* Switzerland: Springer Nature, **2008**.
10. Blankenshi R.E. *Molecular Mechanisms of Photosynthesis*. Chichester: John Wiley & Sons, **2008**.
11. Deisenhofer J., Norris J.R. *Photosynthetic Reaction Center,* Vol. 2, San Diego, CA: Academic Press, **2013**.
12. Barber J. *Chem. Soc. Rev.* **2009**, *38*, 185−196.
13. *Multiporphyrin Arrays: Fundamentals and Applications* (Kim D., Ed.) Singapore: Pan Stanford Publishing Pte. Ltd., **2012**. Ch. 5, 217–288.
14. *Handbook of Porphyrin Science (With Applications to Chemistry, Physics, Material Science, Engineering, Biology and Medicine), Vols. 1 “Supramolecular Chemistry”,*

4 "Phototherapy, Radioimunotherapy and Imaging", 10 "Catalysis and Bio-Inspired Systems" (Kadish K., Smith K.M., Guilard R., Eds.), Abingdon UK: World Scientific Publishing UK Ltd., **2010**.
15. Colvin M.T., Ricks A.B., Scott A.M., Smeigh A., Carmieli R., Miura T., Wasielewski M.R. *J. Am. Chem. Soc*. **2011**, *133*, 1240–1243.
16. Otsuki J., Okumura T., Sugawa K., , Kawano S., Tanaka K., Hirao T., Haino T., Lee Y.J., Kang S., Kim D. *Chem. Eur. J.* **2021**, *27*, 4053–4063.
17. Caballero R., Barrejón M., Cerdá J., Aragó J., Seetharaman S., de la Cruz P., Ortí E., D'Souza F., Langa F. *J. Am. Chem. Soc*. **2021**, *143*, 11199−11208.
18. Sarkar R., Habib M., Kovalenko S.M., Pal S., Prezhdo O.V. *J. Phys. Chem. C* **2021**, *125*, 16620–16628.
19. Brixner T., Hildner R., Köhler J., Lambert C., Würthner F. *Adv. Energy Mater.* **2017**, *7*, 1700236.
20. Cassano D., Voliani V. *Behaviors and Persistence of Nanomaterials in Biomedical Applications*. Scrivener Publishing LLC. John Wiley & Sons, Inc., **2018**.
21. Rabiee N., Yaraki M.T., Garakani S.M., Garakani M., Ahmadi S. Lajevardi A., Bagherzadeh M., Rabiee M., Tayebi L., Tahriri M., Hamblin M.R. *Biomaterials* **2020**, *232*, 119707.
22. Cook L.P., Brewer G., Wong-Ng W. *Crystals* **2017**, *7*(7), 223.
23. De-Jing Li, Qiao-hong Li, Zhi-Gang Gu, Jian Zhang. *Nano Lett*. **2021**, *21*, 10012−10018.
24. Enakieva Y.Y., Zhigileva E.A., Fitch A.N., Chernyshev V.V., Stenina I.A., Yaroslavtsev A.B., Sinelshchikova A.A., Kovalenko K.A., Gorbunova Y.G., Tsivadze A.Yu. *Dalton Trans.* **2021**, *50*, 6549–6560.
25. Schwarz F.P., Gouterman M., Muljiami Z., Dolphin D. *Bioinorg. Chem*. **1972**, *2*(2), 1–32.
26. Gouterman M., Holten D., Liberman E. *Chem. Phys*. **1977**, *25*, 139–153.
27. Anton J.A., Loach P.A. *Photochem. Photobiol*. **1978**, *28*, 235–242.
28. Selenski R., Holten D., Windsor M.V., Pain III J.B., Dolphin D., Gouterman M., Thomas J.C. *Chem. Phys*. **1981**, *60*, 33–46.
29. Overfield R.E., Scherz A., Kaufman K.J., Wasielewski M.R. *J. Am. Chem. Soc*. **1983**, *105*, 5747–5752.
30. Bogatskii A.V., Zhilina Z.I. *Russ. Chem. Rev.* **1982**, *51*, 592–604.
31. Ponomarev G.V., Shulga A.M. *Doklady Akad. Nauk SSSR* **1983**, *271*(2), 365–367.
32. Zenkevich E.I., Shulga A.M., Sagun E.I., Gurinovich G.P. *Materials of All-Union Meeting on Spectroscopy, Part III "Spectroscopy of Complex Molecules"*, Tomsk, **1983**, 102–104.
33. Ponomarev G.V., Shul'ga A.M. *Chem. Heterocycl. Compd*. **1986**, *22*, 228–229.
34. Shul'ga A.M., Ponomarev G.V. *Chem. Heterocycl. Compd*. **1988**, *24*, 276–280.
35. Ponomarev G.V., Borovkov V.V., Sugiura K., Sakata Y., Shulga A.M. *Tetrahedron*. **1993**, *34*, 2153–2156.
36. Zenkevich E.I., Shulga A.M., Sagun E.I., Gurinovich G.P., Chernook A.V. *Teubner-Texte fuhr Physik*, Band 4. Leipzig. BSB B.G. Teubner Verlagsgesselschaft. **1985**, 297–300.
37. Zenkevich E.I., Shulga A.M., Chernook A.V., Gurinovich G.P. *Chem. Phys. Lett.* **1984**, *109*, 306–311.
38. Gurinovich G.P., Zenkevich E.I., Sagun E.I., Shulga A.M. *Opt. Spectrosc*. **1984**, *56*(6), 1037–1043.
39. Gurinovich G.P., Zenkevich E.I., Shulga A.M., Sagun E.I., Mauring K., Suisalu A. *J. Appl. Spectrosc.* **1984**, *41*, 1044–1051.
40. Zenkevich E.I., Shulga A.M., Gurinovich G.P., Sagun E.I., Chernook A.V. *J. Appl. Spectrosc.* **1985**, *42*, 139–144.
41. Zenkevich E.I., Shulga A.M., Sagun E.I., Chernook A.V., Gurinovich G.P. *J. Appl. Spectrosc.* **1985**, *43*(3), 455–461.
42. Zenkevich E.I., Shulga A.M., Chernook A.V., Gurinovich G.P. *J. Appl. Spectrosc.* **1986**, *45*(5), 790–796.
43. Zenkevich E.I., Shulga A.M., Chernook A.V., Gurinovich G.P. *J. Appl. Spectrosc.* **1986**, *45*(6), 984–991.
44. Zenkevich E.I., Shulga A.M., Chernook A.V., Gurinovich G.P. *Khim. Fizika* **1987**, *6*, 1212–1219.
45. Zenkevich E.I., Shulga A.M., Chernook A.V., Sagun E.I., Gurinovich G.P. *Khim. Fizika* **1989**, *8*, 842–853.
46. Zenkevich E.I., Shulga A.M., Chernook A.V., Filatov I.V., Gurinovich G.P. *Theor. Exp. Chem*. **1989**, *25*(3), 295–305.
47. Zenkevich E.I., Chernook A.V., Shulga A.M., Sagun E.I., Gurinovich G.P. *Khim.* **1989**, *8*(7), 891–901.
48. Zenkevich E.I., Chernook A.V., Shulga A.M., Pershukevich P.P., Gurinovich G.P., Sagun E.I. *Khim. Fizika* **1991**, *10,* 1183–1191.
49. Mauring K., Suisalu A., Kikas J., Zenkevich E.I., Chernook A.V., Shulga A.M., Gurinovich G.P. *J. Luminesc*. **1995**, *64*, 141–148.
50. Knyukshto V.N., Sagun E.I., Shulga A.M., Bachilo S.M., Zenkevich E.I. *J. Appl. Spectrosc.* **1998**, *65*, 487–491.
51. Starukhin A.S., Zenkevich E.I., Shulga A.M., Chernook A.V. *J. Luminesc.* **1996**, *68*, 313–323.
52. Knyukshto V.N., Sagun E.I., Shulga A.M., Bachilo S.M., Zenkevich E.I. *Khim. Fizika* **1999**, *8*(5), 30–39.
53. Knyukshto V.N., Zenkevich E.I. Sagun E.I., Shulga A.M., Bachilo S.M. *J. Appl. Spectrosc.* **1999**, *66*, 588–592.
54. Wasielewski M.R. *Chem. Rev*. **1992**, *92*(3), 435–461.
55. Zenkevich E.I., von Borczyskowski C. Multiporphyrin self-assembled arrays in solutions and films: Thermodynamics, spectroscopy and photochemistry. In: *Handbook of Polyelectrolytes and Their Applications* (Tripathy S.K., Kumar, J., Nalwa H.S., Eds.) USA: American Scientific Publishers, **2002**, Vol. 2, Ch. 11, 301–348.
56. Rempel U., von Maltzan B., von Borczyskowski C. *J. Lumin*. **1991**, *48&49*, 415–420.
57. Rempel U., von Maltzan B., von Borczyskowski C. *Pure Appl. Chem*. **1993**, *65*, 1681–1687.
58. Zenkevich E.I., Shulga A.M., Chernook A.V., Rempel U., von Borczyskowski C. *Proc. SPIE 2370, 5th International Conference on Laser Applications in Life Sciences* (2 January 1995), 126–130.
59. Chernook A.V., Shulga A.M., Zenkevich E.I., Rempel U., von Borczyskowski C. *J. Phys. Chem*. **1996**, *100*, 1918–1926.
60. Bachilo S., Willert A., Rempel U., Shulga A.M., Zenkevich E.I., von Borczyskowski C. *J. Photochem. Photobiol. A: Chemistry*. **1999**, *126*, 99–112.
61. Chernook A.V., Rempel U., von Borczyskowski C., Zenkevich E.I., Shulga A.M. *Chem. Phys. Lett*. **1996**, *254*, 229–241.
62. Zenkevich E.I., Shulga A.M., Sagun E.I.,. von Borczyskowski C., Rempel U., Chernook A.V. In: *Advances in Porphyrin Chemistry* [*Uspekhi Khimii Porfirinov*] (Golubchikov O.A., Ed.) St.-Petersburg: University Publ. Co. **1997**, Vol. 1, 270–315.
63. Chernook A.V., Shulga A.M.., Zenkevich E.I., Rempel U., von Borczyskowski C. *Ber. Bunsenges. Phys. Chem*. **1996**, *100*, 114–118.
64. Rempel U., Meyer S., von Maltzan B., von Borczyskowski C. *J. Lumin*. **1998**, *78*, 97–102.
65. Zenkevich E.I., Shulga A.M., Bachilo S.M., Chernook A.V., Rempel U., von Borczyskowski C. *Optika i Spectroskopiya (Opt. Spectrosc.)* **1997**, *83*, 545–655.
66. Zenkevich E.I., Bachilo S.M., Shulga A.M., Rempel U., Willert A., von Borczyskowski C. *Mol. Cryst. Liq. Cryst.* **1998**, *324*, 169–176.
67. Zenkevich E.I., Willert A., Bachilo S.M., Rempel U., Kilin D.S., Shulga A.M., von Borczyskowski C. *Materials Science*

and Engineering C. **2001**, 18(1–2), 99–111.
68. Zenkevich E.I., von Borczyskowski C., Shulga A.M., Bachilo S.M., Rempel U., Willert A. *Chem. Phys*. **2002**, *275*, 185–209.
69. Zenkevich E.I., von Borczyskowski C., Shulga A.M. *J. Porphyrins Phthalocyanines* **2003**, *7*, 731–754.
70. Zenkevich E.I. *Macroheterocycles* **2016**, *9*, 121–140.
71. Zenkevich E.I., Kilin D., von Borczyskowski C., Zahn D.R.T. *Macroheterocycles* **2020**, *13*, 130–141.
72. Zenkevich E., Cichos F., Shulga A., Petrov E., Blaudeck T., von Borczyskowski C. *J. Phys. Chem. B* **2005**, *109*, 8679–8692.
73. Zenkevich E.I., Blaudeck T., Shulga A.M., Cichos F., von Borczyskowski C. *Int. J. Photoenergy* **2006**, *2006*, 090242.
74. Zenkevich E.I., Blaudeck T., Shulga A.M., Cichos F., von Borczyskowski C. *J. Lumin.* **2007**, *122–123*, 784–788.
75. Whitesides G.M., Grzybowski B. *Science* **2002**, *295*, 2418–2421.
76. Kilin D.S., Tsemekhman K., Prezhdo O.V., Zenkevich E.I., von Borczyskowski C. *J. Photochem. Photobiol. A: Chemistry* **2007**, *190*, 342–354.
77. Blaudeck T., Zenkevich E., Cichos F., von Borczyskowski C. *J. Phys. Chem. C* **2008**, *112*, 20251–20257.
78. Zenkevich E.I., von Borczyskowski C. *Macroheterocycles* **2009**, *2*, 206–220.
79. Zenkevich E.I., Stupak A.P., Kowerko D., von Borczyskowski C *Chem. Phys*. **2012**, *406*, 21–29.
80. Zenkevich E.I., Blaudeck T., Kowerko D., Stupak A.P., Cichos F., von Borczyskowski C. *Macroheterocycles* **2012**, *5,* 98–114.
81. Zenkevich E.I., Gaponenko S.V., Sagun E.I., von Borczyskowski C. *Reviews in Nanoscience and Nanotechnology* (Chen W., Zhao Y., P. Juzenas, Eds.) USA: American Scientific Publishers. **2013**, *2*, No 3, 184–207.
82. Zenkevich E., Stupak A., Göhler C., Krasselt C., von Borczyskowski C. *ACS Nano* **2015**, *9*(3), 2886–2903.
83. Stupak A., Blaudeck T., Zenkevich E., Krause S., von Borczyskowski C. *Phys. Chem. Chem. Phys*. **2018**, *20*, 18579–18600.
84. Zenkevich E.I., Blaudeck T., von Borczyskowski C., Zahn D.R.T. *Macroheterocycles* **2020**, *13*, 351–358.
85. Solovyov K.N., Gladkov L.L., Starukhin A S., Shkirman S.F. *Spectroscopy of Porphyrins: Vibrational States*. Minsk: Nauka i Tekhnika, **1985**, 415 p. (in Russ.).
86. Jankowiak R., Reppert M., Zazubovich V., Pieper J., Reinot T. *Chem. Rev.* **2011**, *111,* 4546–4598.
87. Reinot T., Zazubovich V., Hayes J.M., Small G.J. *J. Phys. Chem. B* **2001**, *105,* 5083–5098.
88. Bopp M.A., Sytnik A., Howard T.D., Cogdell R.J., Hochstrasser R.M. *Proc. Natl. Acad. Sci. USA*, **1999**, *96*, 11271–11276.
89. Zenkevich E.I., Shulga A.M., Bachilo S.M., Rempel U., von Richthofen J., von Borczyskowski C. *J. Luminesc*. **1998**, *76&77*, 354–358.
90. Rodriguez J., Kirmaier C., Johnson M.R., Friesner R.A., Holten D., Sessler J.L. *J. Am. Chem. Soc*. **1991**, *113*, 1652–1659.
91. Bixon M., Jortner J., Michel-Beyerle M.E. *Chem. Phys*. **1995**, *197*, 389–404.
92. Kilin D., Kleinekathofer U., Schreiber M. *J. Phys. Chem. A* **2000**, *104*, 5413–5421.
93. Basche T., Moerner W.E., Orrit M., Wild U.P. *Single-Molecule Optical Detection. Imaging and Spectroscopy*. VCH Publishers, **1996**.
94. Moerner W.E. J. *Phys. Chem. B* **2002**, *106,* 910–927.
95. Hartzler D.A., Slipchenko L.V., Savikhin S. *J. Phys. Chem. A* **2018**, *122*, 6713–6723.

Received 20.11.2021
Accepted 25.12.2021